J. Math. Biol.
DOI 10.1007/s00285-012-0629-3

Mathematical Biology

"Classical" Electropermeabilization Modeling at the Cell Scale

Otared Kavian · Michael Leguèbe · Clair Poignard · Lisl Weynans

Received: 11 July 2012 / Revised: 7 November 2012

Abstract The aim of this paper is to provide new models of cell electropermeabilization involving only a few parameters. A static and a dynamical model, which are based on the description of the electric potential in a biological cell, are derived. Existence and uniqueness results are provided for each differential system, and an accurate numerical method to compute the solution is described. We then present numerical simulations that corroborate the experimental observations, providing the consistency of the modeling. We emphasize that our new models involve very few parameters, compared with the most achieved models of Neu and Krassowska (Phys Rev E 53(3):3471–3482, 1999) and DeBruin and Krassowska (Biophys J 77:1225–1233, 1999), but they provide the same qualitative results. Thus, these models will facilitate drastically the forthcoming inverse problem solving, which will consist in fitting them with the experiments.

This research has been partly granted by the French national agency throughout the research projects INTCELL (2010-BLAN-916-04) and MEMOVE (2011-BS01-006-01).

O. Kavian
Département de Mathématiques, LMV CNRS UMR 8100,
Université Versailles-Saint-Quentin, 45 avenue des Etats-Unis,
78035 Versailles Cedex, France

M. Leguèbe · C. Poignard (✉)
INRIA Bordeaux-Sud Ouest (team MC2), IMB CNRS UMR 5251,
Université de Bordeaux, 351, cours de la Libération,
33405 Talence Cedex, France
e-mail: clair.poignard@inria.fr

L. Weynans
Université de Bordeaux, IMB CNRS UMR CNRS 5251,
INRIA Bordeaux-Sud Ouest (team MC2), 351, cours de la Libération,
33405 Talence Cedex, France

Published online: 13 December 2012

Keywords Cell modeling · Non-linear partial differential equations · Finite differences on cartesian grids

Mathematics Subject Classification 92B05 · 35Q92 · 35Q60 · 92C05 · 65N06

1 Introduction

The distribution of the electric potential in a biological cell is important for bio-electromagnetic investigations. A sufficiently large magnitude of the difference of transmembrane potential (denoted from now on by ΔTMP), which is the difference of the electric potentials between both sides of the cell membrane, leads to an increase of the membrane permeability (Pucihar et al. 2006; Teissié et al. 2005). Molecules such as bleomycin can then diffuse across the plasma membrane. This phenomenon, called electropermeabilization, has already been used in oncology and holds promises in gene therapy (Marty et al. 2006; Serša 2005), motivating precise assessments of the ΔTMP.

In this paper, we aim at studying theoretically and numerically two non-linear electrical models (a static and a dynamical model) of biological cells. These models are inspired from the static model of Ivorra et al. (2010). They describe the behavior of both electric potential and membrane conductivity when the cell is submitted to an electric pulse through a few parameters that will be fitted with the experiments. The inverse problem solving to calibrate the models, which is the main goal of this research, is not tackled in the present paper. This article is a first step, in which we present, and study theoretically and numerically new models with a few parameters, in order to simplify the forthcoming inverse problem solving. We emphasize these models are phenomenological in the sense that the membrane conductivity is described by an ad hoc law, which does not come from an homogenization of the nanoscale phenomena. Before stating the model we are going to study, we now detail the notation of the paper.

Notation 1 *Throughout this article, we shall use the following conventions and notation:*

- *We generically denote by* $\mathbf{n}$ *the normal to a closed smooth surface of* $\mathbb{R}^3$ *(or a curve of* $\mathbb{R}^2$*) outwardly directed from the inside to the outside of the domain enclosed by the surface.*
- *Let* $\mathcal{C}$ *be a surface embedded in* $\mathbb{R}^3$*, and let* u *be a sufficiently smooth function (in an appropriate sense) defined in a tubular neighborhood of* $\mathcal{C}$*. We define* $u_{|_{\mathcal{C}^\pm}}$ *by*

$$\forall x \in \mathcal{C}, \quad u_{|_{\mathcal{C}^\pm}}(x) = \lim_{\tau \to 0^+} u(x \pm \tau \mathbf{n}(x)).$$

The notation $\partial_{\mathbf{n}} u_{|_{\mathcal{C}^\pm}}$ *and* $\partial_{\mathbf{t}} u_{|_{\mathcal{C}^\pm}}$ *stands for the normal and the tangential components of* ∇u*:*

$$\forall x \in \mathcal{C}, \quad \partial_{\mathbf{n}} u_{|_{\mathcal{C}^\pm}}(x) = \lim_{\tau \to 0^+} \nabla u(x \pm \tau \mathbf{n}(x)) \cdot \mathbf{n}(x),$$
$$\partial_{\mathbf{t}} u_{|_{\mathcal{C}^\pm}}(x) = \nabla u(x) - \partial_{\mathbf{n}} u(x) \mathbf{n}(x),$$

where the dot " · " denotes the Euclidean scalar product of $\mathbb{R}^3$*. In the case of* $\mathbb{R}^2$*, the analogous notation is easily adapted.*

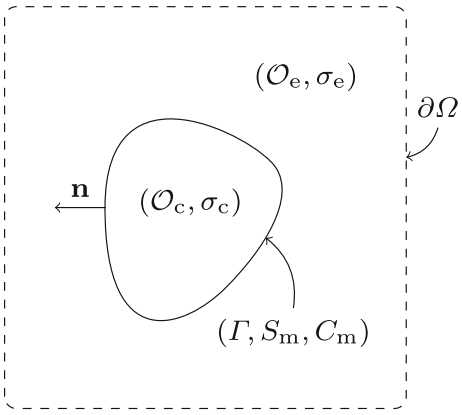

Fig. 1 Geometry of the problem. The cell $\mathcal{O}_c$ is imbedded in the bath $\mathcal{O}_e$. The whole domain Ω is defined by $\Omega = \mathcal{O}_e \cup \overline{\mathcal{O}_c}$

– *The jump* $[u]_{\mathcal{C}}$ *of a function* u *defined in a neighborhood of the surface* $\mathcal{C}$ *is defined by*

$$[u]_{\mathcal{C}} = u|_{\mathcal{C}^+} - u|_{\mathcal{C}^-}.$$

1.1 Electric potential in a biological cell

A biological cell is a high contrast medium composed of a conducting cytoplasm $\mathcal{O}_c$ surrounded by a thin and very insulating layer, embedded in a bath $\mathcal{O}_e$ (see Fig. 1). The plasma membrane is a phospholipid bilayer, which is sprinkled over with proteins. Due to its thickness and its electrical properties, the membrane can be modeled as a surface electric material Γ with a capacity C_m and a surface conductivity S_m. We refer to the seminal articles of Hodgkin et al. for the electric description of cell membranes (Goldman 1943; Hodgkin and Katz 1949; Hodgkin and Huxley 1952; Hodgkin and Horowicz 1959). Let σ be the conductivity of the medium, that is

$$\sigma = \begin{cases} \sigma_e, & \text{in the exterior domain } \mathcal{O}_e, \\ \sigma_c, & \text{inside the cell } \mathcal{O}_c. \end{cases}$$

As described by Neu and Krassowska (1999) and DeBruin and Krassowska (1999a) the electric potential in the whole cell is the discontinuous solution U to the following problem:

$$\Delta U = 0, \quad \text{in } \mathcal{O}_e \cup \mathcal{O}_c, \tag{1a}$$
$$U(0, \cdot) = 0, \quad \text{and for all } t > 0, \tag{1b}$$
$$U(t, x) = g(t, x), \quad \text{on } \partial\Omega, \tag{1c}$$

with the transmission conditions across the membrane Γ:

$$[\sigma \partial_{\mathbf{n}} U]_{\Gamma} = 0, \tag{1d}$$

$$C_{\mathrm{m}}\partial_t [U]_\Gamma + S_{\mathrm{m}} [U]_\Gamma = \sigma_{\mathrm{c}} \partial_{\mathbf{n}} U_{|_{\Gamma^-}}. \tag{1e}$$

Throughout, the paper we denote by Ω the Lipschitz domain

$$\Omega = \mathcal{O}_{\mathrm{e}} \cup \overline{\mathcal{O}_{\mathrm{c}}}$$

and $\partial\Omega$ denotes its boundary. Moreover we define $PH^1(\Omega)$ as

$$PH^1(\Omega) = \left\{ u \in L^2(\Omega) \,:\, u|_{\mathcal{O}_{\mathrm{e}}} \in H^1(\mathcal{O}_{\mathrm{e}}),\, u|_{\mathcal{O}_{\mathrm{c}}} \in H^1(\mathcal{O}_{\mathrm{c}}) \right\},$$

and

$$PH^1_0(\Omega) = \left\{ u \in PH^1(\Omega) \,:\, u|_{\partial\Omega} = 0 \right\}.$$

1.2 Electropermeabilization phenomenon

When submitted to a high electric pulse—i.e. if the magnitude of the pulse g reaches a threshold value—the cell membrane permeability increases and large molecules that usually cannot diffuse through the plasma membrane (for instance, plasmids or bleomycin) enter inside the cytoplasm. This phenomenon is called *electroporation* or *electropermeabilization*. For several years, different membrane models based on hydrodynamic, elasticity, hydroelasticity, viscoelasticity, or aqueous pore formation have been developed to describe the pore formation on the cell membrane [for more details, see the review of Pavlin et al. (2008)]. They all highlight a threshold value of the electric potential above which the electropermeabilization phenomenon occurs. However, the critical potential value changes with the models. Theoretical biophysicists consider the aqueous pore formation model as the most convincing current explanation. Nevertheless, the predictions of the model do not coincide with experiments either quantitatively or phenomenologically since no pore has ever been observed. In addition, the models based on the paper of Neu and Krassowska (1999), DeBruin and Krassowska (1999a,b) are too complex to be parameterized to fit the experiments. Roughly speaking, the current models provide a qualitative explanation of the electropermeabilization, but the problem of the quantitative description remains open.

Actually in vitro and in vivo experiments have never proved the electropore formation, which theoretically could reach detectable size [since macropores could be created according to Smith et al. (2004)]; and it seems unclear whether electroporation results from holes punched in a lipid bilayer, as proposed in the current models (Teissié et al. 2005; Teissié 2005). Moreover, the experimentally proved reversible process of the membrane electroporation is not clearly explained by the current models. In addition, and this is probably one of the main features of the experiments, the *vectorization* of large molecules requires both short time high-voltage pulses and long time low-voltage pulses (André and Gehl 2008). Therefore, the presence of pores is still controversial despite structural changes of the membrane. For all these reasons, we prefer the term *electropermeabilization* to *electroporation*.

1.3 Modeling principle

The probably most achieved electropermeabilization model has been proposed by Neu and Krassowska (1999) and precisely described by DeBruin and Krassowska (1999a,b). It consists in adding an electroporation current I_{ep} in the right-hand side of Eq. (1e):

$$C_{\mathrm{m}}\partial_t [U]_{\Gamma} + S_{\mathrm{m}} [U]_{\Gamma} = \sigma_{\mathrm{c}} \partial_{\mathbf{n}} U_{|_{\Gamma^-}} + I_{\mathrm{ep}}.$$

The current I_{ep} is given by a highly non-linear pore current i_{ep} multiplied by the pore density N_{ep}. The main drawback of such a model is its complexity since several parameters, such as the pore radius or the relative entrance length of the pore, which cannot be measured. Moreover, the mathematical well-posedness of the equations cannot be clearly established. Therefore, the inverse problem, that consists in fitting the parameters for each cell species, is hardly unsolvable numerically. In addition, the "philosophy" of the modeling is based on the pore creation, while as hinted above the very existence of these pores is controversial. For all these reasons, we choose to present here a new phenomenological model of electropermeabilization that could be fitted with the experiments. This model describes the membrane resealing and the memory of the applied pulses.

Our electropermeabilization modeling consists in describing the membrane permeabilization by choosing an appropriate function for the surface conductivity S_{m}, instead of adding an electroporation current based on the pore creation as Neu, Krassowska, et al. did (see Neu and Krassowska 1999, 2006; DeBruin and Krassowska 1999a; Smith et al. 2004). In addition, we propose two models: the first one is a "static" model that describes the electropermeabilization as being an instantaneous phenomenon for a single time-constant pulse. This can be seen as a preliminary model that describes the cell potential during the pulse. The second model is the time-dependent model of electropermeabilization. For each model, we present the theoretical results that ensure existence and uniqueness of the solution to the new problems and then we present the numerical methods that allow the computation of the equations. We conclude by comparing our model with the model of Neu, Krassowska, et al.

2 The static equation

Based on the extensive review of Ivorra et al. (2010), the surface conductivity S_{m} is a function of the absolute membrane voltage, which tends to the value S_{L} (the lipid surface conductivity) below a certain threshold V_{rev} (the reversible electropermeabilization voltage) and tends to S_{ir} (the surface conductivity of the irreversibly electropermeabilized region) above this threshold, with S_{ir} being larger than S_{L}. The "speed of the switch" between these two values is given by a parameter k_{ep}. We may choose the following sigmoid function for S_{m}:

$$\forall \lambda \in \mathbb{R}, \quad S_{\mathrm{m}}(\lambda) = S_{\mathrm{L}} + (S_{\mathrm{ir}} - S_{\mathrm{L}})[1 + \tanh(k_{\mathrm{ep}}(|\lambda| - V_{\mathrm{rev}}))]/2, \tag{2}$$

however other functions with similar monotonicity properties can be considered. More precisely, in our model the function S_{m} will satisfy the following condition:

$$\left.\begin{array}{l} S_{\mathrm{m}} \in C(\mathbb{R}),\ \lambda \mapsto S_{\mathrm{m}}(\lambda) \text{ is even on } \mathbb{R}, \\ 0 < S_{\mathrm{L}} \leq S_{\mathrm{m}}(\lambda) \leq S_{\mathrm{ir}}, \quad S_{\mathrm{m}} \text{ is non decreasing on } [0, +\infty), \\ \lim\limits_{\lambda \to +\infty} S_{\mathrm{m}}(\lambda) = S_{\mathrm{ir}}. \end{array}\right\} \tag{3}$$

In particular, note that the mapping $\lambda \mapsto \lambda S_{\mathrm{m}}(\lambda)$ is increasing on $\mathbb{R}$.

Therefore, the static potential U satisfies the following problem:

$$\Delta U = 0, \quad \text{in } \mathcal{O}_{\mathrm{e}} \cup \mathcal{O}_{\mathrm{c}}, \tag{4a}$$

$$[\sigma \partial_{\mathbf{n}} U]_{\Gamma} = 0, \quad \text{on } \Gamma, \tag{4b}$$

$$S_{\mathrm{m}}([U]_{\Gamma})\,[U]_{\Gamma} = \sigma_{\mathrm{c}} \partial_{\mathbf{n}} U_{|_{\Gamma^-}}, \quad \text{on } \Gamma, \tag{4c}$$

$$U = g \quad \text{on } \partial\Omega. \tag{4d}$$

Remark 2 Model (4) can be seen as the limit of the model of Ivorra et al. (2010), when the membrane thickness tends to zero [we refer to Perrussel and Poignard (2011) for asymptotic expansion of the voltage potential in high contrast medium with resistive thin layer].

In the following subsections, we study the non-linear problem (4). In particular, we emphasize that due to the non-linearity of the membrane conductivity, increasing numerically the thickness of the membrane (as performed in Ivorra et al. 2010) leads to irrelevant results from the quantitative point of view. Therefore, we aim at providing efficient numerical methods in order to solve the above problem.

2.1 Existence and uniqueness of the static potential

This subsection is devoted to the proof of the following result.

Theorem 3 *Let $g \in H^{1/2}(\partial\Omega)$. There exists a unique U satisfying problem (4). This solution satisfies*

$$U_{|\mathcal{O}_e} \in H^1(\mathcal{O}_e), \quad U_{|\mathcal{O}_c} \in H^2(\mathcal{O}_c).$$

In order to prove this theorem, we proceed as follows. Denote by Λ_{c} and Λ_{e} the Dirichlet-to-Neumann operators on Γ (also called Steklov–Poincaré operators) for the Laplacian respectively in $\mathcal{O}_{\mathrm{c}}$ and in $\mathcal{O}_{\mathrm{e}}$. More precisely, denote by $\mathbf{n}_{\mathrm{c}}$ (*resp.* $\mathbf{n}_{\mathrm{e}}$) the unitary outward normal to Γ directed from the inside to the outside of $\mathcal{O}_{\mathrm{c}}$ (*resp.* $\mathcal{O}_{\mathrm{e}}$). We define the operators Λ_{c} and Λ_{e} from $H^{1/2}(\Gamma)$ to $H^{-1/2}(\Gamma)$ as:

$$\forall f \in H^{1/2}(\Gamma), \quad \Lambda_{\mathrm{c}}(f) := \mathbf{n}_{\mathrm{c}} \cdot \sigma_{\mathrm{c}} \nabla v_{\mathrm{c}_{|\Gamma^-}}, \text{ where } \operatorname{div}(\sigma_{\mathrm{c}} \nabla v_{\mathrm{c}}) = 0 \text{ in } \mathcal{O}_{\mathrm{c}}, \text{ and } v_{\mathrm{c}_{|\Gamma}} = f, \tag{5a}$$

$$\Lambda_{\mathrm{e}}(f) := \mathbf{n}_{\mathrm{e}} \cdot \sigma_{\mathrm{e}} \nabla v_{\mathrm{e}_{|\Gamma^+}}, \text{ where } \operatorname{div}(\sigma_{\mathrm{e}} \nabla v_{\mathrm{e}}) = 0 \text{ in } \mathcal{O}_{\mathrm{e}}, \ v_{\mathrm{e}_{|\partial\Omega}} = 0 \text{ and } v_{\mathrm{e}_{|\Gamma}} = f. \tag{5b}$$

Observe that using Wirtinger–Poincaré's inequality in the case of Λ_{c}, or Poincaré's inequality in the case of Λ_{e}, together with the continuity of the mapping $u \mapsto u_{|\partial\mathcal{O}}$ from $H^1(\mathcal{O})$ into $H^{1/2}(\partial\mathcal{O})$, when $\mathcal{O}$ is sufficiently smooth, the following inequalities hold:

$$\langle \Lambda_{\mathrm{c}} f, f \rangle = \int_{\mathcal{O}_{\mathrm{c}}} \sigma_{\mathrm{c}}(x) \nabla v(x) \cdot \nabla v(x) \, \mathrm{d}x \geq C_{\mathrm{c}} \, \| f - M(f) \|^2_{H^{1/2}(\Gamma)}, \tag{6}$$

$$\langle \Lambda_{\mathrm{e}} f, f \rangle = \int_{\mathcal{O}_{\mathrm{e}}} \sigma_{\mathrm{e}}(x) \nabla v_{\mathrm{e}}(x) \cdot \nabla v_{\mathrm{e}}(x) \, \mathrm{d}x \geq C_{\mathrm{e}} \| f \|^2_{H^{1/2}(\Gamma)}, \tag{7}$$

where $M(f) = |\Gamma|^{-1} \int_\Gamma f(\tau) \, \mathrm{d}\tau$ is the mean value of f on Γ, and C_{e} and C_{c} are constants depending only on $\mathcal{O}_{\mathrm{e}}$ and $\mathcal{O}_{\mathrm{c}}$ respectively. Moreover, for a function $g \in H^{1/2}(\partial\Omega)$, we define $\Lambda_0(g)$ by:

$$\Lambda_0(g) := \mathbf{n}_{\mathrm{e}} \cdot \sigma_{\mathrm{e}} \nabla v_{|\Gamma^+}, \quad \text{where } \operatorname{div}(\sigma_{\mathrm{e}} \nabla v) = 0 \text{ in } \mathcal{O}_{\mathrm{e}}, \quad v_{|\partial\Omega} = g \text{ and } v_{|\Gamma} = 0. \tag{8}$$

It is useful to recall that the operator Λ_{e} is invertible, its inverse being given by another Steklov–Poincaré operator (or what is sometimes called a Neumann-to-Dirichlet operator). Namely, for any $\psi \in H^{-1/2}(\Gamma)$ given, one has $\Lambda_{\mathrm{e}}^{-1}(\psi) = v_{|\Gamma}$ where $v \in H^1(\mathcal{O}_{\mathrm{e}})$ satisfies the equation

$$\operatorname{div}(\sigma_{\mathrm{e}} \nabla v) = 0 \ \text{ in } \ \mathcal{O}_{\mathrm{e}}, \ v_{|\partial\Omega} = 0 \ \text{ and } \ \mathbf{n}_{\mathrm{e}} \cdot \sigma_{\mathrm{e}} \nabla v_{|\Gamma^+} = \psi.$$

Consider the Hilbert space $\mathbb{H}$ defined by

$$\mathbb{H} = H^{1/2}(\Gamma) \times H^{1/2}(\Gamma),$$

with the norm

$$\forall \, \mathbf{u} = (u_{\mathrm{e}}, u_{\mathrm{c}}) \in \mathbb{H}, \quad \|\mathbf{u}\|^2_{\mathbb{H}} = \|u_{\mathrm{e}}\|^2_{H^{1/2}(\Gamma)} + \|u_{\mathrm{c}}\|^2_{H^{1/2}(\Gamma)}.$$

Problem (4) can be written on the manifold Γ with the help of the above Steklov–Poincaré operators. More precisely, problem (4) is equivalent to finding $(u_{\mathrm{e}}, u_{\mathrm{c}}) \in \mathbb{H}$ such that

$$\begin{aligned} \Lambda_{\mathrm{e}} u_{\mathrm{e}} + S_{\mathrm{m}}(u_{\mathrm{e}} - u_{\mathrm{c}})(u_{\mathrm{e}} - u_{\mathrm{c}}) &= -\Lambda_0(g), \\ \Lambda_{\mathrm{c}} u_{\mathrm{c}} - S_{\mathrm{m}}(u_{\mathrm{e}} - u_{\mathrm{c}})(u_{\mathrm{e}} - u_{\mathrm{c}}) &= 0. \end{aligned} \tag{9}$$

Notation 4 *Identifying the dual of $L^2(\Gamma) \times L^2(\Gamma)$ with $L^2(\Gamma) \times L^2(\Gamma)$, we denote by $\mathbb{H}'$ the dual space of $\mathbb{H}$ and by $\langle \cdot\,, \cdot \rangle$ the duality between $\mathbb{H}$ and $\mathbb{H}'$.*

The proof of Theorem 3 is an obvious application of the following theorem.

Theorem 5 *Let $\mathbf{G} = (G_e, G_c) \in \mathbb{H}'$. There exists a unique $\mathbf{u^0} = (u_e, u_c) \in \mathbb{H}$ such that*

$$\begin{aligned} \Lambda_e u_e + S_m(u_e - u_c)(u_e - u_c) &= G_e, \\ \Lambda_c u_c - S_m(u_e - u_c)(u_e - u_c) &= G_c. \end{aligned} \tag{10}$$

Proof We define the operator $\boldsymbol{\Lambda}_\sigma$ from $\mathbb{H}$ into $\mathbb{H}'$ by

$$\forall \mathbf{u} \in \mathbb{H}, \quad \boldsymbol{\Lambda}_{\boldsymbol{\sigma}} \mathbf{u} = \begin{pmatrix} \Lambda_{\mathrm{e}} u_{\mathrm{e}} \\ \Lambda_{\mathrm{c}} u_{\mathrm{c}} \end{pmatrix} = \begin{pmatrix} \Lambda_{\mathrm{e}} & 0 \\ 0 & \Lambda_{\mathrm{c}} \end{pmatrix} \begin{pmatrix} u_{\mathrm{e}} \\ u_{\mathrm{c}} \end{pmatrix}. \tag{11}$$

Thanks to (6) and (7), we have

$$\forall \mathbf{u} \in \mathbb{H}, \quad \langle \boldsymbol{\Lambda}_{\boldsymbol{\sigma}} \mathbf{u}, \mathbf{u} \rangle \geq C_{\mathrm{e}} \left\| u_{\mathrm{e}} \right\|^2_{H^{1/2}(\Gamma)} + C_{\mathrm{c}} \left\| u_{\mathrm{c}} - M(u_{\mathrm{c}}) \right\|^2_{H^{1/2}(\Gamma)}. \tag{12}$$

Since the function S_{m} satisfies conditions (3), we introduce the function F defined by

$$\forall\, s \in \mathbb{R}, \quad F(s) = \int_0^s S_{\mathrm{m}}(z) z \, \mathrm{d}z.$$

Note that F is even, that is $F(-s) = F(s)$. Let $\mathbf{J_1}$ be the function defined on $\mathbb{H}$ by

$$\forall \mathbf{u} \in \mathbb{H}, \quad \mathbf{J_1}(\mathbf{u}) = \mathbf{J_1}(u_{\mathrm{e}}, u_{\mathrm{c}}) = \int_\Gamma F(u_{\mathrm{e}}(\tau) - u_{\mathrm{c}}(\tau)) \, \mathrm{d}\tau.$$

One easily checks that $\mathbf{J_1}$ is a C^1 function on $\mathbb{H}$ and

$$\mathbf{J_1}(\mathbf{u}) \geq \frac{1}{2} S_{\mathrm{L}} \int_\Gamma |u_{\mathrm{e}}(\tau) - u_{\mathrm{c}}(\tau)|^2 \, \mathrm{d}\tau.$$

Observe that, for any $\mathbf{u} \in \mathbb{H}$, the derivative $\mathbf{J_1'}(\mathbf{u})$ of $\mathbf{J_1}$ at $\mathbf{u}$ is the linear map defined by

$$\forall\, \mathbf{h} \in \mathbb{H}, \quad \mathbf{J_1'}(\mathbf{u}) \cdot \mathbf{h} = \int_\Gamma S_m\big(u_{\mathrm{e}}(\tau) - u_{\mathrm{c}}(\tau)\big)(u_{\mathrm{e}}(\tau) - u_{\mathrm{c}}(\tau))(h_{\mathrm{e}}(\tau) - h_{\mathrm{c}}(\tau)) \, \mathrm{d}\tau.$$

Let $\mathbf{J}$ be defined by

$$\forall \mathbf{u} \in \mathbb{H}, \quad \mathbf{J}(\mathbf{u}) = \frac{1}{2}\langle \mathbf{\Lambda}_{\boldsymbol{\sigma}} \mathbf{u} \rangle + \mathbf{J_1}(\mathbf{u}) - \langle \mathbf{G}, \mathbf{u} \rangle.$$

$\mathbf{J}$ is of class $\mathscr{C}^1$ on $\mathbb{H}$ and $\mathbf{J}'$ is given by

$$\forall\, \mathbf{u} \in \mathbb{H}, \quad \mathbf{J}'(\mathbf{u}) = \begin{pmatrix} \Lambda_{\mathrm{e}} u_{\mathrm{e}} + S_{\mathrm{m}}(u_{\mathrm{e}} - u_{\mathrm{c}})(u_{\mathrm{e}} - u_{\mathrm{c}}) - G_{\mathrm{e}} \\ \Lambda_{\mathrm{c}} u_{\mathrm{c}} - S_{\mathrm{m}}(u_{\mathrm{e}} - u_{\mathrm{c}})(u_{\mathrm{e}} - u_{\mathrm{c}}) - G_{\mathrm{c}} \end{pmatrix}. \tag{13}$$

In order to show that $\mathbf{J}'$ is a monotone operator, we define the nonlinear operator B from $\mathbb{H}^2$ into $\mathbb{R}$ by

$$\forall (\mathbf{u}, \mathbf{v}) \in \mathbb{H}^2, \quad B(\mathbf{u}, \mathbf{v}) = S_{\mathrm{m}}([\mathbf{u}])[\mathbf{u}]^2 \left(1 - \frac{[\mathbf{v}]}{[\mathbf{u}]}\right)\left(1 - \frac{S_{\mathrm{m}}([\mathbf{v}])}{S_{\mathrm{m}}([\mathbf{u}])}\frac{[\mathbf{v}]}{[\mathbf{u}]}\right), \tag{14}$$

where for simplicity we denote by $[\mathbf{u}] = u_{\mathrm{e}} - u_{\mathrm{c}}$ for $\mathbf{u} = (u_{\mathrm{e}}, u_{\mathrm{c}}) \in \mathbb{H}$. Taking into account the fact that S_{m} satisfies (3), one checks easily that $B(\mathbf{u}, \mathbf{v}) \geq 0$. According to (12) and (13), for $(\mathbf{u}, \mathbf{v}) \in \mathbb{H}^2$ we have

$$\langle \mathbf{J}'(\mathbf{u}) - \mathbf{J}'(\mathbf{v}), \mathbf{u} - \mathbf{v} \rangle = \langle \mathbf{\Lambda}_{\boldsymbol{\sigma}}(\mathbf{u} - \mathbf{v}), \mathbf{u} - \mathbf{v} \rangle + \int_{\Gamma} B\big(\mathbf{u}(s), \mathbf{v}(s)\big)\, \mathrm{d}s, \tag{15}$$

from which we infer that $\mathbf{J}'$ is a monotone operator. Therefore $\mathbf{J}$ is convex. In order to see the strict convexity of $\mathbf{J}$, that is the strict monotonicity of $\mathbf{J}'$, we have to show that if for a given $\mathbf{u}, \mathbf{v} \in \mathbb{H}$ we have $\langle \mathbf{J}'(\mathbf{u}) - \mathbf{J}'(\mathbf{v}), \mathbf{u} - \mathbf{v} \rangle = 0$, then we have $\mathbf{u} = \mathbf{v}$. Observe first that, since $\lambda \mapsto \lambda S_{\mathrm{m}}(\lambda)$ is increasing, we have that

$$B(\mathbf{u}, \mathbf{v}) = 0 \quad \Longrightarrow \quad [\mathbf{u}] = [\mathbf{v}].$$

In particular, for these $\mathbf{u}, \mathbf{v}$, we have $B(\mathbf{u}, \mathbf{v}) = 0$, which implies $[\mathbf{u}] = [\mathbf{v}]$, hence $u_{\mathrm{e}} - v_{\mathrm{e}} = u_{\mathrm{c}} - v_{\mathrm{c}}$. On the other hand, since

$$\langle \Lambda_{\mathrm{e}}(u_{\mathrm{e}} - v_{\mathrm{e}}), u_{\mathrm{e}} - v_{\mathrm{e}} \rangle = \langle \Lambda_{\mathrm{c}}(u_{\mathrm{c}} - v_{\mathrm{c}}), u_{\mathrm{c}} - v_{\mathrm{c}} \rangle = 0,$$

and since Λ_{e} is coercive, we conclude that $u_{\mathrm{e}} - v_{\mathrm{e}} = 0$, which in turn implies that $u_{\mathrm{c}} - v_{\mathrm{c}} = 0$. Finally, this shows that

$$\langle \mathbf{J}'(\mathbf{u}) - \mathbf{J}'(\mathbf{v}), \mathbf{u} - \mathbf{v} \rangle = 0 \quad \Longrightarrow \quad \mathbf{u} = \mathbf{v}.$$

Therefore, $\mathbf{J}'$ is strictly monotone and $\mathbf{J}$ is strictly convex.

In order to show the coerciveness of $\mathbf{J}$, that is $\mathbf{J}(\mathbf{u}) \to +\infty$ when $\|\mathbf{u}\|_{\mathbb{H}} \to \infty$, we proceed as follows. Observe first that

$$\begin{aligned}|\langle G_{\mathrm{c}}, M(u_{\mathrm{c}})\rangle| &\leq \|G_{\mathrm{c}}\|_{H^{-1/2}(\Gamma)}\, \|M(u_{\mathrm{e}}-u_{\mathrm{c}})\|_{H^{1/2}(\Gamma)} \\ &\quad + \|G_{\mathrm{c}}\|_{H^{-1/2}(\Gamma)}\, \|M(u_{\mathrm{e}})\|_{H^{1/2}(\Gamma)}\,, \\ &\leq \|G_{\mathrm{c}}\|_{H^{-1/2}(\Gamma)}\, \|M(u_{\mathrm{e}}-u_{\mathrm{c}})\|_{H^{1/2}(\Gamma)} \\ &\quad + \|G_{\mathrm{c}}\|_{H^{-1/2}(\Gamma)}\, \|u_{\mathrm{e}}\|_{H^{1/2}(\Gamma)}\,,\end{aligned}$$

hence

$$\begin{aligned}|\langle \mathbf{G}, \mathbf{u}\rangle| &\leq \left(\|G_{\mathrm{e}}\|_{H^{-1/2}(\Gamma)} + \|G_{\mathrm{c}}\|_{H^{-1/2}(\Gamma)}\right) \|u_{\mathrm{e}}\|_{H^{1/2}(\Gamma)} \\ &\quad + \|G_{\mathrm{c}}\|_{H^{-1/2}(\Gamma)}\, \|u_{\mathrm{c}} - M(u_{\mathrm{c}})\|_{H^{1/2}(\Gamma)} \\ &\quad + \|G_{\mathrm{c}}\|_{H^{-1/2}(\Gamma)}\, \|M(u_{\mathrm{e}}-u_{\mathrm{c}})\|_{H^{1/2}(\Gamma)}\,.\end{aligned}$$

Using Young's inequality ($ab \leq \varepsilon a^2 + C(\varepsilon)b^2$, for $\varepsilon > 0$ and $C(\varepsilon) := (4\varepsilon)^{-1}$) we infer

$$\begin{aligned}|\langle \mathbf{G}, \mathbf{u}\rangle| &\leq \varepsilon\, \|u_{\mathrm{e}}\|^2_{H^{1/2}(\Gamma)} + \varepsilon\, \|u_{\mathrm{c}} - M(u_{\mathrm{c}})\|^2_{H^{1/2}(\Gamma)} + 2\, C(\varepsilon)\|\mathbf{G}\|^2_{\mathbb{H}'} \\ &\quad + \|G_{\mathrm{c}}\|_{H^{-1/2}(\Gamma)}\, \|M(u_{\mathrm{e}}-u_{\mathrm{c}})\|_{H^{1/2}(\Gamma)}\,. \end{aligned} \tag{16}$$

On the other hand, using the fact that $2F(s) \geq S_{\mathrm{L}} s^2$ for $s \in \mathbb{R}$, we deduce that

$$\begin{aligned}\mathbf{J_1}(\mathbf{u}) &\geq \frac{1}{2} S_{\mathrm{L}} \int_{\Gamma} |u_{\mathrm{e}}(\tau) - u_{\mathrm{c}}(\tau)|^2 \mathrm{d}\tau \\ &\geq \frac{1}{2} S_{\mathrm{L}} \left(\int_{\Gamma} |(u_{\mathrm{e}}-u_{\mathrm{c}}) - M(u_{\mathrm{e}}-u_{\mathrm{c}})|^2 \mathrm{d}\tau + \int_{\Gamma} |M(u_{\mathrm{e}}-u_{\mathrm{c}})|^2 \mathrm{d}\tau \right).\end{aligned}$$

Using this inequality, together with (16), we obtain a lower bound for $\mathbf{J}(\mathbf{u})$ (here $a(\varepsilon), C(\varepsilon)$ are positive constants depending on the arbitrary $\varepsilon > 0$, and $b > 0$ is a constant):

$$\begin{aligned}\mathbf{J}(\mathbf{u}) &\geq a(\varepsilon) \left(\|u_{\mathrm{e}}\|^2_{H^{1/2}(\Gamma)} + \|u_{\mathrm{c}} - M(u_{\mathrm{c}})\|^2_{H^{1/2}(\Gamma)} \right) \\ &\quad + b \int_{\Gamma} |M(u_{\mathrm{e}}-u_{\mathrm{c}})|^2 \mathrm{d}\tau - \|G_{\mathrm{c}}\|_{H^{-1/2}(\Gamma)}\, \|M(u_{\mathrm{e}}-u_{\mathrm{c}})\|_{H^{1/2}(\Gamma)} \\ &\quad - C(\varepsilon)\|\mathbf{G}\|^2_{\mathbb{H}'}.\end{aligned} \tag{17}$$

Since $M(u_{\mathrm{e}} - u_{\mathrm{c}})$ is a constant, we observe that one has $\|M(u_{\mathrm{e}} - u_{\mathrm{c}})\|_{H^{1/2}(\Gamma)} = c_* \|M(u_{\mathrm{e}} - u_{\mathrm{c}})\|_{L^2(\Gamma)}$ for some positive constant c_* independent of $\mathbf{u}$. Consequently, for any $\varepsilon > 0$ so that $b - \varepsilon > 0$, there exists a constant $c(\varepsilon)$ such that

$$b\int_{\Gamma}|M(u_{\mathrm{e}}-u_{\mathrm{c}})|^2\mathrm{d}\tau-\|G_{\mathrm{c}}\|_{H^{-1/2}(\Gamma)}\,\|M(u_{\mathrm{e}}-u_{\mathrm{c}})\|_{H^{1/2}(\Gamma)}$$
$$\geq(b-\varepsilon)\|M(u_{\mathrm{e}}-u_{\mathrm{c}})\|^2_{H^{1/2}(\Gamma)}-c(\varepsilon)\|G_{\mathrm{c}}\|^2_{H^{-1/2}(\Gamma)}.$$

Using this inequality in the lower bound (17), we conclude that

$$\lim_{\|\mathbf{u}\|_{\mathbb{H}}\to+\infty}\mathbf{J}(\mathbf{u})=+\infty$$

hence $\mathbf{J}$ achieves its minimum at a unique point $\mathbf{u^0}\in\mathbb{H}$, which satisfies Eq. (10). □

3 The dynamical model

In this section, we focus on the dynamical description of the electropermeabilization. Our model is based on the description of two quantities: the time-dependent electric potential and the ratio of the electropermeabilized region over the total membrane area, which is also time-dependent. In Sect. 3.1, we present the main considerations that lead to our model. We then study its solvability: existence and uniqueness results are presented in Sect. 3.4.

3.1 Heuristics of the modeling

Experimental observations suggest that the permeabilization process at a certain location depends on whether the membrane conductivity is above a certain threshold or not. This leads us to define the surface membrane conductivity as an interpolation between the two values S_{ir} and S_{L}, the interpolation parameter $\xi(t,s)\in[0,1]$ being itself a function of time and of the point s on the membrane Γ. In our interpretation, the parameter $\xi(t,s)$ measures in some way the likelihood that a given infinitesimal portion of the membrane is going to be electropermeabilized. More precisely, when $\xi(t,s)$ equals 0 at a given point $s\in\Gamma$, the membrane conductivity equals the lipid conductivity at this point (thus there is no electropermeabilization), while for $\xi(t,s)=1$ it corresponds to the maximal value of the membrane surface conductivity above which electropermeabilization is irreversible. Thus the time-dependent membrane conductivity, denoted by S_{m} writes

$$\forall(t,s)\in(0,+\infty)\times\Gamma,\quad S_{\mathrm{m}}(t,s)=S_{\mathrm{L}}+\xi(t,s)(S_{\mathrm{ir}}-S_{\mathrm{L}}).\tag{18}$$

On the other hand, the changes in the conductivity at a certain location $s\in\Gamma$ depend on the transmembrane voltage. Denoting by $[\mathbf{u}]:=u_{\mathrm{e}}-u_{\mathrm{c}}$ the *jump* in the potential between the outside and the inside of the cell for $\mathbf{u}:=(u_{\mathrm{e}},u_{\mathrm{c}})\in\mathbb{H}$ (as we did in the previous sections), we therefore assume that

$$\xi(t,s)=X(t,[\mathbf{u}(t,s)]),\tag{19}$$

where the function $(t,\lambda)\mapsto X(t,\lambda)$ will be defined below.

The main idea of the modeling consists in writing a differential equation that describes the dynamics of $(t, \lambda) \mapsto X(t, \lambda)$ similarly to a *sliding door* model. Let β be a function satisfying

$$\left.\begin{array}{l} \beta \in W^{1,\infty}(\mathbb{R}),\ \lambda \mapsto \beta(\lambda) \text{ is even on } \mathbb{R}, \\ \lambda \mapsto \lambda\beta'(\lambda) \quad \text{belongs to } L^{\infty}(\mathbb{R}), \\ 0 \leq \beta(\lambda) \leq 1, \quad \beta \text{ is non decreasing on } (0, +\infty), \\ \lim\limits_{\lambda \to +\infty} \beta(\lambda) = 1. \end{array}\right\} \tag{20}$$

An example of such a function would be

$$\forall \lambda \in \mathbb{R}, \qquad \beta(\lambda) := (1 + \tanh(k_{\text{ep}}(|\lambda| - V_{\text{rev}}))/2.$$

Let us describe now the evolution of X. For $\lambda_0 \in \mathbb{R}$, which will stand for a given ΔTMP, and for an initial value $X_0 \in [0, 1]$ of X, set $\beta_0 := \beta(\lambda_0)$. Then we consider the following two possibilities:

- Either $\beta_0 - X_0$ is positive, in which case the electric pulse is sufficiently high to enlarge the electropermeabilized region, with a *characteristic time of electropermeabilization* of order τ_{ep}.
- Or $\beta_0 - X_0$ is negative, in which case we consider that the pulse is not high enough to increase the electropermeabilization. Therefore, the membrane *tries to reseal* with a characteristic *resealing* time of order τ_{vres}. Since experimental observations suggest that this phenomenon takes much more time than the electropermeabilization process, we assume that $\tau_{\text{vres}} > \tau_{\text{ep}}$.

Remark that when a cell is at rest, X_0 equals zero, but if high voltage pulses have been applied earlier than the initial time, X_0 might not be equal to zero.

Based on these considerations, for any $\lambda_0 \in \mathbb{R}$, we assume that $X(\cdot, \lambda_0)$ satisfies the following differential equation:

$$\begin{cases} \frac{\partial X}{\partial t}(t, \lambda_0) = \max\left(\frac{\beta(\lambda_0) - X(t,\lambda_0)}{\tau_{\text{ep}}}\ ;\ \frac{\beta(\lambda_0) - X(t,\lambda_0)}{\tau_{\text{res}}}\right), \qquad \forall t > 0, \\ X(0, \lambda_0) = X_0. \end{cases} \tag{21}$$

3.2 Statement of the mathematical problem

We first write the equation satisfied by the potential U defined on the domain $\mathcal{O}_{\text{e}} \cup \mathcal{O}_{\text{c}}$. We assume that before the imposition of the electrical pulses g on the external boundary $\partial\Omega$, the cell potential is at rest and given by $U_0 \in H^1(\Omega)$. This resting potential translates the ionic exchanges through the membrane. According to equalities (18)–(19), the membrane conductivity $\widetilde{S}_{\text{m}}$ is defined by:

$$\widetilde{S}_{\text{m}}(t, \lambda) := S_{\text{L}} + (S_{\text{ir}} - S_{\text{L}})X(t, \lambda). \tag{22}$$

We seek the solution (U, X) to the following system of equations: for (U_0, X_0) given, the pair of functions (U, X) satisfy:

$$
\begin{aligned}
&U|_{t=0} = U_0, \quad \text{and for any } t > 0,\\
&\Delta U = 0, \quad \text{in } (0,T)\times(\mathcal{O}_e \cup \mathcal{O}_c), \quad U(t,\cdot) = g(t,\cdot) \quad \text{on } (0,+\infty)\times\partial\Omega, && \text{(23a)}\\
&[\sigma\partial_{\mathbf{n}} U] = 0, \quad \text{on } (0,T)\times\Gamma, && \text{(23b)}\\
&C_m\partial_t[U](t,\cdot) + \widetilde{S}_m(t,[U])[U] = \sigma_c\partial_{\mathbf{n}}U(t,\cdot)_{|\Gamma^-}, \quad \text{on } (0,T)\times\Gamma, && \text{(23c)}
\end{aligned}
$$

where, writing $\lambda = [U](t,s)$, the function X appearing in (22) satisfies the differential equation

$$
\begin{aligned}
&\frac{\partial X(t,\lambda)}{\partial t} = \max\left(\frac{\beta(\lambda) - X(t,\lambda)}{\tau_{ep}}; \frac{\beta(\lambda) - X(t,\lambda)}{\tau_{vres}}\right), \quad t > 0, && \text{(24a)}\\
&X(0,\lambda) = X_0. && \text{(24b)}
\end{aligned}
$$

Remark 6 Observe that if the source g does not depend on the time t, the stationary point (U^*, X^*) of the system (23)–(24a) is the unique solution to

$$
\begin{aligned}
&\Delta U^* = 0, \quad \text{in } (\mathcal{O}_e \cup \mathcal{O}_c), \qquad U^*|_{\partial\Omega} = g \qquad \text{on } \partial\Omega,\\
&[\sigma\partial_{\mathbf{n}} U^*] = 0, \quad \text{on } \Gamma,\\
&\left(S_L + (S_{ir} - S_L)X^*\right)[U^*] = \sigma_c\partial_{\mathbf{n}}U^*_{|\Gamma^-}, \quad \text{on } \Gamma,
\end{aligned}
$$

where

$$
X^* = \beta([U^*(s)]),
$$

which coincides with the static model (2).

3.3 Properties of the function X

Let us state the following lemma regarding the solution to Eq. (24):

Lemma 7 *Let $T > 0$ be fixed and let β satisfy condition (20). For $T > 0$ and any $\lambda \in \mathbb{R}$, the following differential equation*

$$
\begin{cases}
\frac{\partial X(t,\lambda)}{\partial t} = \max\left(\frac{\beta(\lambda) - X(t,\lambda)}{\tau_{ep}}; \frac{\beta(\lambda) - X(t,\lambda)}{\tau_{vres}}\right), \quad \forall t \in (0,T),\\
X(0,\lambda) = X_0 \in [0,1],
\end{cases}
\tag{25}
$$

has a unique solution $X(\cdot,\lambda) \in C^1([0,T])$. Moreover one has

$$
0 \le X(t,\lambda) = X(t,-\lambda) = X(t,|\lambda|) \le 1, \qquad \forall t \in [0,T], \quad \forall \lambda \in \mathbb{R}.
$$

In addition, there exists a constant $K(T) > 0$ such that for any $\lambda_1, \lambda_2 \in \mathbb{R}$ we have

$$\forall t \in [0, T], \quad |\lambda_1 X(t, \lambda_1) - \lambda_2 X(t, \lambda_2)| \leq K(T) \, |\lambda_1 - \lambda_2| \, . \tag{26}$$

Proof The mapping $X \mapsto \max([\beta(\lambda) - X]/\tau_{\text{ep}}, [\beta(\lambda) - X]/\tau_{\text{vres}})$, defined from $\mathbb{R}$ into itself, is clearly Lipschitz for all fixed λ. Therefore, the differential Eq. (25) has a unique solution $X \in C^1([0, T])$, for any given $X_0 \in \mathbb{R}$.

Assuming now that $0 \leq X_0 \leq 1$, multiplying the Eq. (25) by $X^- := \max(-X, 0)$, and using the fact that $\beta \geq 0$, one gets

$$\frac{1}{2} \partial_t |X^-|^2 \leq 0.$$

Thus $X^-(\cdot, \lambda) \equiv 0$ on $[0, T]$. Similarly, using the fact that $\beta - 1 \leq 0$, and multiplying the equation by $(X - 1)^+ = \max(X - 1, 0)$, one sees that

$$\partial_t |(X - 1)^+|^2 \leq 0,$$

and finally $0 \leq X(t, \lambda) \leq 1$, for any $t \in [0, T]$.

In order to show the estimate (26), we proceed as follows. For $\lambda \in \mathbb{R}$ denote by $Y(t, \lambda) := \lambda X(t, \lambda)$. Since for any $(a, b) \in \mathbb{R}$, we have $\max(a, b) = a + (a - b)^-$, assuming for instance that $\tau_{\text{ep}} < \tau_{\text{vres}}$ we observe that

$$\max(a/\tau_{\text{ep}}, a/\tau_{\text{vres}}) = \frac{a}{\tau_{\text{ep}}} + \left(\tau_{\text{ep}}^{-1} - \tau_{\text{vres}}^{-1}\right) a^-,$$

and using the equality $a^- = (|a| - a)/2$ we get

$$\max(a/\tau_{\text{ep}}, a/\tau_{\text{vres}}) = a \left(\tau_{\text{ep}}^{-1} + \tau_{\text{vres}}^{-1}\right)/2 + |a| \left(\tau_{\text{ep}}^{-1} - \tau_{\text{vres}}^{-1}\right)/2.$$

From this we induce that Y satisfies the following O.D.E

$$\begin{cases} \frac{\partial Y(t,\cdot)}{\partial t} = H(\lambda, Y), \quad \forall t \in (0, T), \\ Y(0, \lambda) = Y_0 = \lambda X_0, \end{cases} \tag{27}$$

where the function H is defined by

$$H : (\lambda, Y) \mapsto H(\lambda, Y) = (\lambda\beta(\lambda) - Y) \left(\tau_{\text{ep}}^{-1} + \tau_{\text{vres}}^{-1}\right)/2 + \lambda \, |\beta(\lambda) - Y/\lambda| \left(\tau_{\text{ep}}^{-1} - \tau_{\text{vres}}^{-1}\right)/2. \tag{28}$$

In order to see that the mapping $\lambda \mapsto H(\lambda, Y)$ is globally Lipschitz on $\mathbb{R}$, since by our assumptions on the function β we know that $\lambda\beta'(\lambda)$ is uniformly bounded on $\mathbb{R}$, the function $\lambda \mapsto \lambda\beta(\lambda)$ is Lipschitz on $\mathbb{R}$, and thus we have only to verify that the

function $h : \lambda \mapsto h(\lambda, Y) = \lambda\,|\beta(\lambda) - Y/\lambda|$ is Lipschitz on $\mathbb{R}$. Indeed, this is the case as one can see by a simple computation that

$$\begin{aligned}\frac{\partial h}{\partial \lambda} &= |\beta(\lambda) - Y/\lambda| + (\lambda\beta'(\lambda) + Y/\lambda)\frac{\beta(\lambda) - Y/\lambda}{|\beta(\lambda) - Y/\lambda|},\\ &= \left(\beta(\lambda) + \lambda\beta'(\lambda)\right)\frac{\beta(\lambda) - Y/\lambda}{|\beta(\lambda) - Y/\lambda|},\end{aligned}$$

and therefore

$$\left|\frac{\partial h}{\partial \lambda}(\lambda, Y)\right| \leq \left|\beta(\lambda) + \lambda\beta'(\lambda)\right|.$$

From this, one infers clearly that the mapping $(\lambda, Y) \mapsto H(\lambda, Y)$ is globally Lipschitz on $\mathbb{R} \times \mathbb{R}$. Writing

$$Y(t, \lambda_1) - Y(t, \lambda_2) = \int_0^t \left(H(\lambda_1, Y_1) - H(\lambda_2, Y_2)\right)(t)dt + (\lambda_1 - \lambda_2)X_0;$$

we conclude that

$$\forall t \in (0, T), \quad |Y(t, \lambda_1) - Y(t, \lambda_2)| \leq K(T)\,|\lambda_1 - \lambda_2|,$$

thanks to an invocation of Gronwall lemma. □

3.4 Existence and uniqueness of the dynamical potential

Since the non-linearity of problem (23) appears in the transmission condition (23c), we are going to rewrite it on the surface Γ using the Steklov–Poincaré operators, in the same manner as we did in the previous section for the static model. We first prove the following property:

Lemma 8 *The operator $\Lambda_e + \Lambda_c$ is positive, selfadjoint and invertible from $H^{1/2}(\Gamma)$ into $H^{-1/2}(\Gamma)$. The operator*

$$\mathcal{B} := Id + \Lambda_e^{-1}\Lambda_c$$

is therefore invertible, from $H^{1/2}(\Gamma)$ into itself.

Moreover, define the domain $D(\Lambda_c\mathcal{B}^{-1})$ as

$$D(\Lambda_c\mathcal{B}^{-1}) = \left\{\varphi \in H^{1/2}(\Gamma) \,:\, \Lambda_c\mathcal{B}^{-1}\varphi \in L^2(\Gamma)\right\}.$$

The operator $\left(\Lambda_c\mathcal{B}^{-1}, D(\Lambda_c\mathcal{B}^{-1})\right)$ is m–accretive (more precisely $D(\Lambda_c\mathcal{B}^{-1}) = H^1(\Gamma)$).

Proof That $\Lambda_e + \Lambda_c$ is invertible is an easy consequence of the fact that the operator Λ_e is a positive, selfadjoint and invertible operator while Λ_c is non-negative and selfadjoint. Thus, $\Lambda_e + \Lambda_c$ is also a positive selfadjoint invertible operator.

Let $\varphi \in D(\Lambda_c \mathcal{B}^{-1})$. Then, by definition (and invertibility) of $\mathcal{B}$ (i.e. $\mathrm{Id} = \left(\mathrm{Id} + \Lambda_e^{-1}\Lambda_c\right)\mathcal{B}^{-1}$) we have

$$\begin{aligned}\langle \Lambda_c \mathcal{B}^{-1}\varphi, \varphi\rangle &= \langle \Lambda_c \mathcal{B}^{-1}\varphi, \varphi\rangle,\\ &= \langle \Lambda_c \mathcal{B}^{-1}\varphi, \mathcal{B}^{-1}\varphi\rangle + \langle \Lambda_c \mathcal{B}^{-1}\varphi, \Lambda_e^{-1}\Lambda_c \mathcal{B}^{-1}\varphi\rangle,\\ &= \langle \Lambda_c \mathcal{B}^{-1}\varphi, \mathcal{B}^{-1}\varphi\rangle + \langle \Lambda_e \Lambda_e^{-1}\Lambda_c \mathcal{B}^{-1}\varphi, \Lambda_e^{-1}\Lambda_c \mathcal{B}^{-1}\varphi\rangle\\ &\geq 0.\end{aligned}$$

$\Lambda_c \mathcal{B}^{-1}$ is therefore accretive. Let $f \in L^2(\Gamma)$, let $\lambda > 0$ and let U be the unique solution in $PH_0^1(\Omega)$ to the following problem:

$$\begin{aligned}&-\Delta U = 0, \text{ in } \mathcal{O}_e \cup \mathcal{O}_c, \quad U_{|\partial\Omega} = 0,\\ &\sigma_e \partial_{\mathbf{n}} U_{|\Gamma^+} = \sigma_c \partial_{\mathbf{n}} U_{|\Gamma^-},\\ &\lambda\sigma_c \partial_{\mathbf{n}} U_{|\Gamma^-} + U_{|\Gamma^-} - U_{|\Gamma^+} = f.\end{aligned}$$

Therefore, setting $v := U_{|\Gamma^-} - U_{|\Gamma^+}$, v satisfies

$$v + \lambda \Lambda_c \mathcal{B}^{-1} v = f.$$

In addition, since $\Lambda_c \mathcal{B}^{-1}$ is nonnegative , we have $\|v\|_{L^2(\Gamma)} \leq \|f\|_{L^2(\Gamma)}$. Therefore, $\Lambda_c \mathcal{B}^{-1}$ is m–accretive. □

Lemma 9 *Let U_0 and X_0 be two enough regular functions defined respectively in Ω and on Γ, and recall that $\widetilde{S}_m(t,\lambda) := S_L + (S_{ir} - S_L)X(t,\lambda)$ is defined in (22). Finding the solution (U, X) to problem (23)–(24), if it exists, is equivalent to finding (u_e, u_c, X), with $u_e = U_{|\Gamma^+}$ and $u_c = U_{|\Gamma^-}$ satisfying:*

$$u_e = u_c - v, \tag{29}$$

$$u_c = \mathcal{B}^{-1}\left(v - \Lambda_e^{-1}\Lambda_0 g\right), \tag{30}$$

where v is the solution to

$$\begin{aligned}&C_m \partial_t v + \Lambda_c \mathcal{B}^{-1} v + \widetilde{S}_m(t, v)v = G,\\ &v(0,\cdot) = \varphi,\end{aligned} \tag{31}$$

with φ and G being defined as

$$\varphi = U_{0|\Gamma^+} - U_{0|\Gamma^-}, \quad G := \Lambda_c \mathcal{B}^{-1}\Lambda_e^{-1}\Lambda_0 g,$$

and where, writing $\lambda = v(t,s), \quad a.e.(t,s) \in (0,T)\times\Gamma$, X *satisfies*

$$\begin{cases} \partial_t X(t,\lambda) = \max\left(\frac{\beta(\lambda)-X(t,\lambda)}{\tau_{ep}}; \frac{\beta(\lambda)-X(t,\lambda)}{\tau_{res}}\right), \quad \forall t > 0, \\ X(0,\lambda) = X_0. \end{cases} \tag{32}$$

Proof The lemma is a straightforward consequence of the definition of the Steklov–Poincaré operators Λ_c, Λ_e, Λ_0, and of the invertibility of Λ_e. Indeed, condition (23b), that is the continuity of the flux across Γ, boils down to

$$\Lambda_\mathrm{e} u_\mathrm{e} + \Lambda_0 g + \Lambda_\mathrm{c} u_\mathrm{c} = 0,$$

from which, thanks to the invertibility of Λ_e, we infer that

$$u_\mathrm{e} - u_\mathrm{c} = -\left(\mathcal{B} u_\mathrm{c} + \Lambda_\mathrm{e}^{-1}\Lambda_0 g\right) = -v.$$

In addition, by definition of v, we have

$$\Lambda_\mathrm{c} u_\mathrm{c} = \Lambda_\mathrm{c}\mathcal{B}^{-1} v - \Lambda_\mathrm{c}\mathcal{B}^{-1}\Lambda_\mathrm{e}^{-1}\Lambda_0 g = \Lambda_\mathrm{c}\mathcal{B}^{-1} v - G.$$

Then, the transmission condition (23c) [multiplied by (-1)] reads (31), provided we recall that β is an even function and that $\widetilde{S}_m$ is defined by (22). □

We now show that the evolution equations appearing in Lemma 9 have a unique solution.

Theorem 10 *Assume that* β *satisfies* (20), $G \in L^p((0,T); L^2(\Gamma))$ *for some* $p > 1$, *and that* $\varphi \in L^2(\Gamma)$ *is given. Let* $X_0 \in L^\infty(\Gamma)$ *such that* $0 \le X_0 \le 1$ *on* Γ, *and let* $\widetilde{S}_m$ *be defined as in* (22).

Then, there exists a unique function $v \in C([0,T]; L^2(\Gamma))$, *mild solution to the system*

$$\begin{cases} C_m \partial_t v + \Lambda_c \mathcal{B}^{-1} v + \widetilde{S}_m(t,v)v = G, \quad \forall t \in (0,T), \\ v(0) = \varphi, \end{cases} \tag{33}$$

where $\widetilde{S}_m$ *is given by* (22), *and writing* $\lambda = v(t,s), \quad a.e\,(t,s) \in (0,T)\times\Gamma$, *one has*

$$\begin{cases} \partial_t X(t,\lambda) = \max\left(\frac{\beta(\lambda)-X(t,\lambda)}{\tau_{ep}}; \frac{\beta(\lambda)-X(t,\lambda)}{\tau_{res}}\right), \quad \forall t \in (0,T), \\ X(0,\lambda) = X_0. \end{cases} \tag{34}$$

Moreover, if $\varphi \in H^1(\Gamma)$ *and* $G \in W^{1,1}((0,T); L^2(\Gamma))$, *the above mild solution is a classical solution to* (33), *in the sense that*

$$v \in C([0,T]; H^1(\Gamma)) \cap C^1([0,T]; L^2(\Gamma)).$$

Proof To simplify the notations we denote by $\mathcal{A}$ the operator

$$\mathcal{A} = \frac{1}{C_{\rm m}} \Lambda_{\rm c} \mathcal{B}^{-1}.$$

In a first step, we are going to show existence and uniqueness of a mild solution to (33) in $C([0,T];L^2(\Gamma))$. Thanks to Lemma 7, we know that for any $\lambda \in \mathbb{R}$, the solution to

$$\begin{cases} \partial_t X(t,\lambda) = \max\left(\frac{\beta(\lambda)-X(t,\lambda)}{\tau_{\rm ep}}; \frac{\beta(\lambda)-X(t,\lambda)}{\tau_{\rm vres}}\right), \forall t > 0, \\ X|_{t=0} = X_0, \end{cases}$$

exists and belongs to $C^1([0,T])$. Moreover, $0 \le X \le 1$, and the mappings $\lambda \mapsto X$ and $\lambda \mapsto \lambda X$ are Lipschitz. Now, upon setting

$$\mathcal{F}(t,v) := -\widetilde{S}_{\rm m}(t,v)v + G = -\left(S_{\rm L} + (S_{\rm ir} - S_{\rm L})X(t,v)\right)v + G,$$

solving equations (33) is equivalent to finding $v \in C([0,T];L^2(\Gamma))$ solution to the following equation, which is the mild version of Eq. (33):

$$v = {\rm e}^{-t\mathcal{A}}\varphi + \frac{1}{C_{\rm m}} \int_0^t \exp\left(-(t-\tau)\mathcal{A}\right) \mathcal{F}(\tau, v) d\tau. \tag{35}$$

Thanks to inequality (26) of Lemma 7, it is clear that the mapping

$$v \mapsto \mathcal{F}(\cdot, v),$$

is Lipschitz from the space

$$\mathbb{E} := C([0,T];L^2(\Gamma))$$

into itself. This means that there exists $K_1 > 0$ such that for any $v, w \in C([0,T];L^2(\Gamma))$ we have

$$\|\mathcal{F}(\cdot,v) - \mathcal{F}(\cdot,w)\|_{L^\infty((0,T);L^2(\Gamma))} \le K_1 \|v-w\|_{L^\infty((0,T);L^2(\Gamma))}.$$

We shall endow the space $\mathbb{E}$ with the norm

$$\|\psi\|_{\mathbb{E}} := \sup_{t\in[0,T]} {\rm e}^{-\alpha t} \|\psi(t,\cdot)\|_{L^2(\Gamma)},$$

for some $\alpha > 0$, which will be chosen below. If we set

$$\Phi(U_{\rm c})(t) := {\rm e}^{-t\mathcal{A}}\varphi + \frac{1}{C_{\rm m}} \int_0^t \exp\left(-(t-\tau)\mathcal{A}\right) \mathcal{F}(\tau, U_{\rm c}(\tau))\, d\tau,$$

then $\Phi : \mathbb{E} \longrightarrow \mathbb{E}$ is a continuous mapping. We shall check that, upon choosing α appropriately, it is a strict contraction. Thus, it has a unique fixed point, providing the unique solution of (35). Indeed

$$\Phi(U_c)(t) - \Phi(V)(t) = \int_0^t \exp\left(-\frac{t-\tau}{C_m}\Lambda_c \mathcal{B}^{-1}\right)[\mathcal{F}(\tau, U_c) - \mathcal{F}(\tau, V)]\, d\tau.$$

Since the operator $\Lambda_c \mathcal{B}^{-1}$ is m–accretive, the operator $\mathcal{A}$ generates a contraction semi-group and the following estimate holds

$$\|e^{-(t-\tau)\mathcal{A}}[\mathcal{F}(\tau, U_c) - \mathcal{F}(\tau, V)]\|_{L^2(\Gamma)} \leq \|[\mathcal{F}(\tau, U_c) - \mathcal{F}(\tau, V)]\|_{L^2(\Gamma)}.$$

Therefore, we infer

$$\begin{aligned}\|\Phi(U_c)(t) - \Phi(V)(t)\|_{L^2(\Gamma)} &\leq \| \int_0^t \|\mathcal{F}(\tau, U_c) - \mathcal{F}(\tau, V)\|_{L^2(\Gamma)}\, d\tau, \\ &\leq K_1 \|U_c - V\|_{\mathbb{E}} \int_0^t e^{\alpha\tau}\, d\tau, \\ &\leq C(p) K_1\, \alpha^{-1}\, e^{\alpha t} \|U_c - V\|_{\mathbb{E}},\end{aligned}$$

from which we conclude that

$$\|\Phi(U_c) - \Phi(V)\|_{\mathbb{E}} \leq \alpha^{-1}\, C(p) K_1\, \|U_c - V\|_{\mathbb{E}}.$$

This implies that for α large enough, the mapping Φ is a strict contraction on $\mathbb{E}$. Equation (33) has thus a unique mild solution in $C([0, T]; L^2(\Gamma))$.

Suppose now that G belongs to $W^{1,1}((0, T); L^2(\Gamma))$ and that $\varphi \in H^1(\Gamma)$. The mild solution given by formula (35) belongs to $C^1([0, T]; L^2(\Gamma))$ hence we infer

$$\partial_t v + \widetilde{S}_m(\cdot, v)v \in C([0, T]; L^2(\Gamma)).$$

Therefore, setting $U_c = U_{|\mathcal{O}_c}$, we have

$$\Delta U_c(t, \cdot) = 0, \text{ in } \mathcal{O}_c, \quad \sigma_c \partial_n U_c(t, \cdot) \in L^2(\Gamma),$$

from which we infer that $U_c(t, \cdot) \in H^{3/2}(\mathcal{O}_c)$. Hence we deduce that since the domains are smooth $U_c(t, \cdot)_{|\Gamma^-}$ belongs to $H^1(\Gamma)$. Similar reasoning for $U_e = U_{|\mathcal{O}_e}$ implies that $U_e(t, \cdot)_{|\Gamma^+}$ belongs to $H^1(\Gamma)$, and therefore the jump v belongs to $C([0, T]; H^1(\Gamma))$, which ends the proof. □

4 Numerical simulations

In this section, we provide some numerical results that show the consistency of our models. In order to solve both static and dynamical problems, we first present the finite-difference method on a cartesian grid adapted from the second-order scheme of Cisternino and Weynans (2012). Note that it is not the scope of this paper to prove rigorously that our scheme is of order two, however numerical simulations of Fig. 3b seems to confirm this order. The rigorous numerical analysis of the method will be performed in a forthcoming work. Since the long-term goal of this work is to fit the models with the experimental data, and since experiments are performed with several thousands of cells per cm^2, parallel computing will be necessary to solve the inverse problem. Therefore, we choose to use accurate schemes on cartesian grids, such as the scheme of Cisternino and Weynans (2012), for which the accuracy has been shown and the parallelization has be already performed, despite Galerkin formulations might be more adapted to the single cell problem, since variational formulation holds.

4.1 Spatial discretization

We perform the discretization on a cartesian grid covering the domain $\Omega = \mathcal{O}_\mathrm{e} \cup \overline{\mathcal{O}_\mathrm{c}}$, which is a square domain of length L (L equals 200 μm for the computations, see Table 1). The interface is described by a level-set function Osher and Sethian (1988), which separates the extra- and intra-cellular domains by the use of a signed distance function φ. The normal to the interface $\mathbf{n}(x)$ outwardly directed from the inner to the outer of the cell is directly obtained by computing numerically $\nabla\varphi(x)$.

The grid spacing is denoted by h, and N is the number of points such as

$$N = L/h.$$

For any $(i, j) \in N^2$ we denote by M_{ij} the grid points defined by

$$M_{i,j} = (x_i, y_j), \quad \text{where} \quad x_i = ih_x,\ y_j = jh_y, \quad \forall (i, j) \in N^2.$$

The numerical approximation of the solution to the static or to the dynamical model at the point (x_i, y_j) is generically denoted by u_{ij}.

Standard approximation of the Laplacian is used in the discretized domains $\mathcal{O}_\mathrm{e}$ and $\mathcal{O}_\mathrm{c}$ far from the interface, which is the cell membrane Γ. However, due to the jump conditions, a special treatment of the approximation of the Laplacian and of the computation of the fluxes is needed at the points nearing the cell membrane.

If the intersection of the interface and $[M_{ij}\ M_{i+1j}]$ exists, then we define the interface point $I_{i+1/2,\,j} = (\tilde{x}_{i+1/2\,,j}, y_j)$ as this intersection. We create two additional unknowns at this interface point, called interface unknowns, and denoted by $\tilde{u}^\mathrm{e}_{i+1/2\,,j}$ and $\tilde{u}^\mathrm{c}_{i+1/2\,,j}$. The interface point $I_{i,\,j+1/2} = (x_i, \tilde{y}_{i,\,j+1/2})$ is similarly defined as the intersection of Γ and the segment $[M_{ij}M_{ij+1}]$.

An example of the discretization method is given by Fig. 2. On regular grid points, that are not neighboring the interface, the Laplacian is discretized with a standard

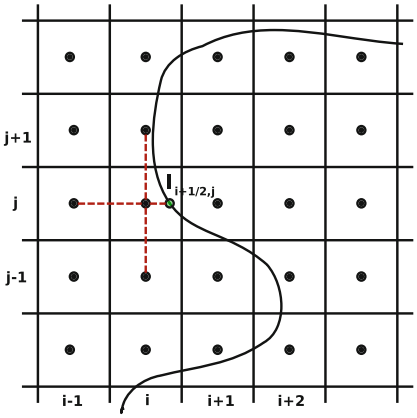

(a) Discretization of the Laplacian on the points at the interface.

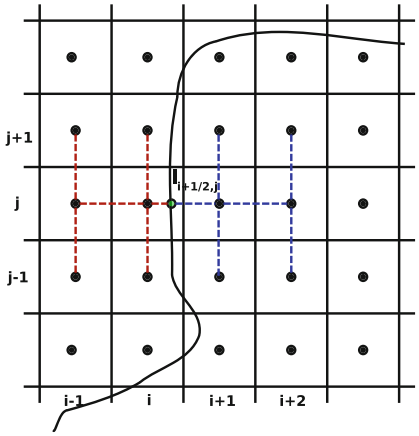

(b) Discretization of ∇U at the interface: non-stabilized stencil.

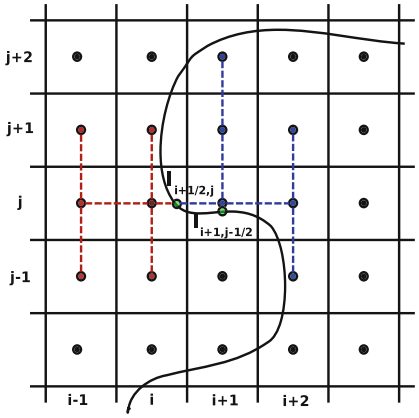

(c) Discretization of ∇U at the interface: stabilized stencil.

Fig. 2 Discretizations of the Laplacian and of the gradient of U at the interface. The first y–derivative stencil on the right side is shifted to avoid an ill-conditioned discretization

centered second-order finite-difference scheme. A specific five points stencil including the interface points is used for neighboring points, as shown in Fig. 2a.

Figure 2b provides an example of the discretization of ∇U on both sides of the interface. The x-derivative of U can be computed with second-order accuracy using a one-sided formula involving three grid points. For example we approximate the flux on the left (for instance exterior) side of the interface with the points $M_{i-1\,j}$, M_{ij} and $I_{i+1/2\,,j}$ by:

$$\frac{\partial U}{\partial x}(\tilde{x},\, y_j) \approx \frac{(u_{i-1\,j} - \tilde{u}^{\mathrm{e}}_{i+1/2\,,j})(x_i - \tilde{x})}{h_x(x_{i-1} - \tilde{x})} - \frac{(u_{ij} - \tilde{u}^{\mathrm{e}}_{i+1/2\,,j})(x_{i-1} - \tilde{x})}{h_x(x_i - \tilde{x})}, \tag{36}$$

where for the sake of brevity, we have replaced $\tilde{x}_{i+1/2\,,j}$ by $\tilde{x}$. The y–derivative cannot be obtained in the same way, since there are no grid points aligned with the interface point in the y–direction. We therefore use a linear combination of $(\partial_y u)_{ij}$ and $(\partial_y u)_{i-1\,j}$, defined respectively as second order approximations of the y–derivative on M_{ij} and $M_{i-1\,j}$. We obtain

$$\frac{\partial U^{\mathrm{e}}}{\partial y}(\tilde{x}, y_j) \approx \frac{\tilde{x} - x_{i-1}}{h_x}\,(\partial_y u)_{ij} - \frac{\tilde{x} - x_i}{h_x}\,(\partial_y u)_{i-1\,j}. \tag{37}$$

The formulas for $(\partial_y u)_{ij}$ and $(\partial_y u)_{i-1\,j}$ depend on the local configuration on the interface, but they are based on the same principle as for (36). The scheme is stabilized by using a shifted y–stencil if two interface points are involved in the same flux discretization, as illustrated by Fig. 2c.

4.2 Accuracy of the finite difference method

In order to show the accuracy of the numerical method, we compare both explicit and numerical solutions to the linear static problem (4), i.e without electroporation. This means that in (4c), S_{m} is constant equal to S_{L}.

Consider a domain composed of two concentric disks. The cell is the disk of radius R_1, centered at 0. The domain Ω is the disk with the same center as the cell, and whose radius R_2 is stricly greater than R_1. The boundary data g equals $E R_2 \cos\theta$, such that the cell is embbeded in a uniform electric field of magnitude E in the x–direction. The exact solution $\widetilde{U}$ to (4) is then explicitely given by

$$\begin{aligned} \forall (r,\theta) \in (R_1, R_2) \times [0, 2\pi], \qquad & \widetilde{U}_{\mathrm{e}}(r,\theta) = (\alpha_{\mathrm{e}} r + \beta_{\mathrm{e}} r^{-1}) \cos\theta, \\ \forall (r,\theta) \in (0, R_1) \times [0, 2\pi], \qquad & \widetilde{U}_{\mathrm{c}}(r,\theta) = \alpha_{\mathrm{c}} r \cos\theta, \end{aligned} \tag{38}$$

where α_{e}, β_{e}, and α_{c} are given by

$$\begin{aligned} \alpha_{\mathrm{c}} &= \left(\left(\frac{\sigma_{\mathrm{c}}}{S_{\mathrm{L}} R_1} + 1 + \frac{\sigma_{\mathrm{c}}}{\sigma_{\mathrm{e}}} \right) R_2 + \left(\frac{\sigma_{\mathrm{c}}}{S_{\mathrm{L}} R_1} + 1 - \frac{\sigma_{\mathrm{c}}}{\sigma_{\mathrm{e}}} \right) \frac{R_1^2}{R_2} \right)^{-1} g, \\ \alpha_{\mathrm{e}} &= \frac{1}{2} \left(\frac{\sigma_{\mathrm{c}}}{S_{\mathrm{L}} R_1} + 1 + \frac{\sigma_{\mathrm{c}}}{\sigma_{\mathrm{e}}} \right) \alpha_{\mathrm{c}}, \\ \beta_{\mathrm{e}} &= \frac{1}{2} \left(\frac{\sigma_{\mathrm{c}}}{S_{\mathrm{L}} R_1} + 1 - \frac{\sigma_{\mathrm{c}}}{\sigma_{\mathrm{e}}} \right) \alpha_{\mathrm{c}} R_1^2. \end{aligned}$$

This analytic solution is projected on the edges of the square Q_L centered at 0, and whose characteristic length L satisfies $R_1 < L/2 < L\sqrt{2}/2 < R_2$ (see Fig. 3a).

In order to verify the accuracy of the space discretization, at least in this configuration, we solve numerically problem (4) in the square Q_L, with the trace $\widetilde{U}|_{\partial Q_L}$ of the analytic solution $\widetilde{U}$ on the edges of Q_L as Dirichlet boundary condition for different grid spacings h. We set the parameters equal to

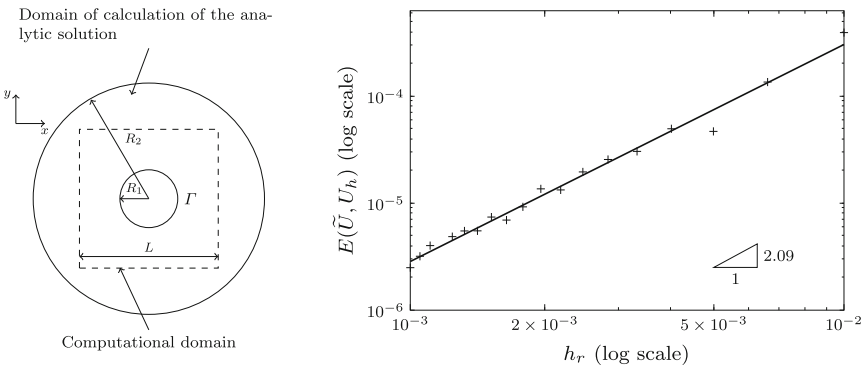

(a) Domains of calculation of the analytic and of the numerical solutions.

(b) Log-log diagram of the error $E(\widetilde{U}, U_h)$ given by (39) with respect to h_r.

Fig. 3 Numerical estimation of the order of accuracy of the method. The analytic solution to the linear problem is calculated in concentric circular domains. The restriction of this solution to the boundary of the computational domain (*dashed line*) provides the Dirichlet data for the numerical solution. Relative error between the two solutions with respect to the grid spacing is plotted in **b**

$$R_2 = 150\ \mu\text{m}, \quad R_1 = 50\ \mu\text{m}, \quad L = 200\ \mu\text{m}, \quad E = 400\ \text{V/cm},$$

the electric parameters being given by Table 1. These parameters come from the values given by DeBruin and Krassowska, see Table 1 of DeBruin and Krassowska (1999a).

We then compare the numerical solution U_h to $\widetilde{U}$. The relative error is computed using both grid and interface points:

$$E(\widetilde{U}, U_h) := \frac{||U_h - \widetilde{U}||_{L^2(\Omega)} + |U_h - \widetilde{U}|_{L^2(\Gamma)}}{||\widetilde{U}||_{L^2(\Omega)} + |\widetilde{U}|_{L^2(\Gamma)}}. \tag{39}$$

We denote by h_r the relative grid spacing defined by

$$h_r = h/L.$$

Figure 3b shows the behavior of $E(\widetilde{U}, U_h)$ with respect to h_r: the space discretization is of order two for this specific case. Note Cisternino and Weynans (2012) have shown the second order accuracy of their method, therefore despite we have adapted the scheme to our problem, we are confident in the good accuracy of the numerical method.

4.3 Computation of the non-linear static model

When solving the static Eq. (4), if one uses the following naive iterative method:

$$S_{\text{m}}([U^n])[U^{n+1}] = \sigma_{\text{c}} \partial_{\mathbf{n}} U_{\text{c}}^{n+1},$$

one finds that the iterative scheme oscillates between two values. This might be a consequence of the fact that the membrane conductivity takes its extreme values S_{L}

Table 1 Parameters set to fit to the results given by Neu and Krassowska (1999), DeBruin and Krassowska (1999a)

Variable	Symbol	Value	Unit
Biological parameters			
Extracellular conductivity	σ_e	5	S/m
Intracellular conductivity	σ_c	0.455	S/m
Capacitance	C_m	9.5×10^{-3}	F/m^2
Membrane surface conductivity	S_L	1.9	S/m^2
Cell radius	r	50	μm
Membrane thickness	δ	5	nm
Specific parameters of the model			
EP threshold	V_{rev}	1,5	V
EP switch speed	k_{ep}	40	V^{-1}
EP characteristic time	τ_{ep}	1×10^{-6}	s
Resealing characteristic time	τ_{vres}	1×10^{-3}	s
EPd membrane surface conductivity	S_{ir}	2.5×10^{8}	S/m^2
Numerical parameters			
Simulation box size	L	200	μm
Grid points (each side)	N	50	
Time step	Δt	20	ns
Pulse duration	T_p	100	μs
Duration of simulation	T_f	150	μs
Number of time steps	N_T	7500	

EP electropermeabilization, *EPd* electropermeabilized

and S_{ir} instead of reaching an intermediate state. Another issue might be that the mapping $\mathcal{L}_g$ defined by

$$\mathcal{L}_g : v \mapsto u,$$

where $u \in PH^1(\Omega)$ is solution to

$$\begin{cases} \Delta u = 0, \quad \text{in } \mathcal{O}_e \cup \mathcal{O}_c, \quad u_{|\partial\Omega} = g, \\ [\sigma \partial_{\mathbf{n}} u]_\Gamma = 0, \quad S_m\big([v]_\Gamma\big)\,[u]_\Gamma = \sigma_c \partial_{\mathbf{n}} u|_\Gamma, \end{cases}$$

is not a contraction, since the Lipschitz constant of S_m is of order $k_{ep} S_m \gg 1$.

We use a modified mapping $\mathcal{L}_{\rho,g}$:

$$\mathcal{L}_{\rho,g} : v \mapsto u,$$

where $u \in PH^1(\Omega)$ is solution to

$$\begin{cases} \Delta u = 0, \quad \text{in } \mathcal{O}_e \cup \mathcal{O}_c, \quad u_{|\partial\Omega} = g, \\ [\sigma \partial_{\mathbf{n}} u]_\Gamma = 0, \quad [u]_\Gamma + \rho S_m\big([v]_\Gamma\big)\,[u]_\Gamma - \rho\sigma_c \partial_{\mathbf{n}} u|_\Gamma = [v]_\Gamma\,, \end{cases}$$

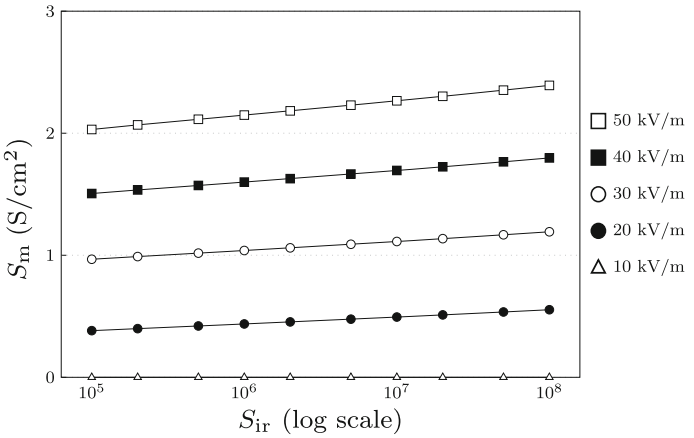

Fig. 4 Membrane surface conductivity S_m at the pole of the cell ($\theta = 0$) obtained by solving the static equation with different values of S_{ir} for pulse magnitudes from 10 to 50 kV/m (the numerical values of the other parameters are given in Table 1)

where ρ is a small positive parameter chosen so as $\mathcal{L}_{\rho,g}$ be a contractive operator. The following iteration process is used:

$$U^0 \text{ given}, \quad \text{and for any } n \geq 0 \quad U^{n+1} = \mathcal{L}_{\rho,g}(U^n).$$

For the simulations we set the stopping criterion of the scheme at $\gamma = 10^{-12}$, meaning that the numerical solution is obtained when the relative error $E(U^{n+1}, U^n)$ is smaller that γ.

4.3.1 Influence of the parameter S_{ir}

The parameter S_{ir}, which is the conductivity of the fully "electroporated" membrane is hardly measurable by the experiments. It is therefore important to investigate its influence on the model. Figure 4 shows that S_{ir} has a little influence on the membrane conductivity S_m, as the value of X counter-balance the variation of S_{ir}. Therefore, the numerical criterion to define the electroporation should involve the parameter S_m.

4.3.2 Comparison with the model of Ivorra, Mir and Villemejeane

We compare our results with the simulations of Ivorra et al. by studying the influence of the extracellular medium conductivity on the membrane conductivity. In Fig. 5, we show results similar to those presented in Fig. 7 of Ivorra et al. (2010). Note that to perform their simulations, Ivorra et al. have multiplied by ten the membrane thickness. This is the reason why their permeabilizing field is of order of magnitude of 2 MV/m, which is much higher than the magnitude used in the experiments, typically (Mir 2001, 2005; Gowrishankar et al. 2006) to the range 20– 30 kV/m. In contrast, our model provides more realistic conditions of electropermeabilization.

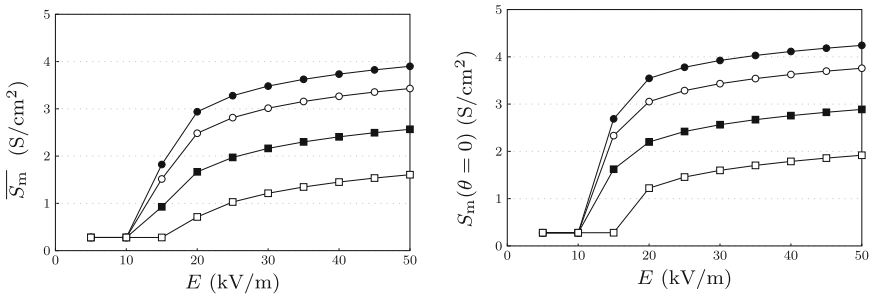

(a) Average value $\overline{S_m}$ of S_m over Γ. **(b)** Pointwise value of S_m at the cell pole.

Fig. 5 Non-linear membrane conductivity of the static model for four different extracellular conductivity: $\sigma_e = 1$ S/m (*filled circle*), $\sigma_e = 0.1$ S/m (*open circle*), $\sigma_e = 0.01$ S/m (*filled square*), $\sigma_e = 0.001$ S/m (*open square*)

4.4 Computation of the dynamical problem

4.4.1 Time-discretization of the model

The time-derivative $\partial_t[U]$ of (23) is discretized using the following scheme:

$$C_m \frac{[U]^{n+1} - [U]^n}{dt} - \sigma_c \partial_{\mathbf{n}} U_c^{n+1} + \widetilde{S}_m(t^n, [U]^n)[U]^n = 0. \tag{40}$$

The Runge-Kutta method of order 4 is used to compute the variable X, with time steps dt.

Figure 6a and b show the numerical results at $t = 100$ µs using the parameters of Table 1. In order to visualize the membrane electropermeabilization, we depict it with boxes, which are colored and sized according to the values of $\widetilde{S}_m$ at each point of Γ and at $t = 100$ µs. We emphasize this is a visualization artefact: in our model, the cell membrane is a surface without any thickness.

4.4.2 Main parameters influence

The key parameters of the model define the electropermeabilization coefficient $\widetilde{S}_m$, that is k_{ep}, V_{rev}, S_{ir} and the characteristic times τ_{ep} and τ_{vres}. A numerical sensitivity analysis was led to determine how the behavior of the solution with respect to a variation of each specific parameter, as shown on Fig. 7. All the parameters defining the function β have a very small influence on the average $\overline{X}$ of X over the cell membrane. Even for small values of k_{ep}, the values of $\overline{X}$ are only modified by a factor 2 (Fig. 7a). On the other hand, the "fully electroporated" membrane conductivity S_{ir}, which was first taken as $(\sigma_c + \sigma_e)/(2\delta)$, affects greatly the order of magnitude of $\overline{X}$, changing from 10^{-6} to 10^{-2} (Fig. 7d). Therefore, as for the static case the relevant quantity to observe the phenomenon is $\widetilde{S}_m$.

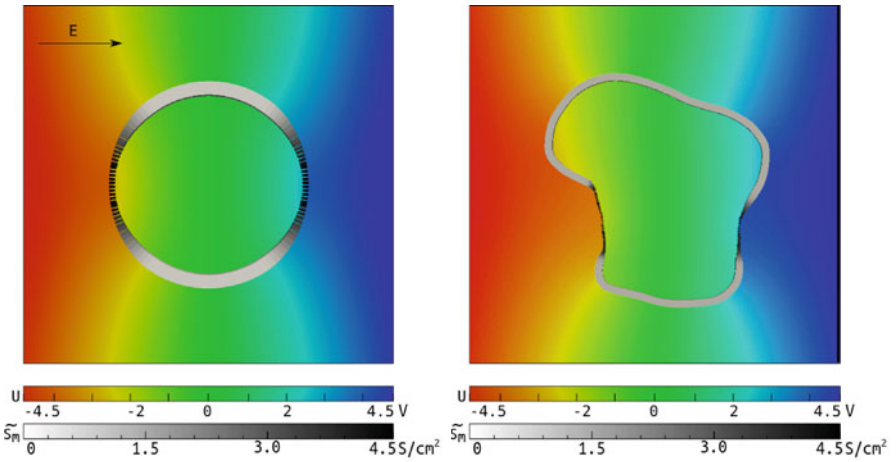

(a) Solution to the dynamical model for a circular cell.

(b) Solution to the dynamical model for a smooth non-convex cell shape.

Fig. 6 Solution to the dynamical problem at the time $t = 100$ µs for two different cell shapes: circular (**a**) and irregular (**b**) shapes. It shows that the electropermeabilized regions depend on the cell shape and the cell orientation with the electric field. The numerical parameters are given in Table 1

4.4.3 Comparison with the model of Neu, Krassowska, and Debruin

The main difference between the model of Neu, Krassowska, et al. and ours resides in the addition of an electroporation current $I_{ep} = N_{ep} i_{ep}$, instead of a direct description of the variations of the surface membrane conductivity $\widetilde{S}_m$.

The equation satisfied by the transmembrane voltage in the model of Neu, Krassowska, et al. (DeBruin and Krassowska 1999a) reads

$$-\sigma_c \partial_n U_c = C_m \partial_t [U] + S_L [U] + N_{ep} i_{ep}, \tag{41}$$

where the ionic reversal currents have been neglected. N_{ep} is the pore density, obeying the ordinary differential equation (parameters are emphasized in bold):

$$\frac{\mathrm{d}N_{ep}}{\mathrm{d}t} = \boldsymbol{\alpha} \mathrm{e}^{([U]/\boldsymbol{V_{rev}})} \left(1 - \frac{N_{ep}}{\boldsymbol{N_0}} \mathrm{e}^{-\boldsymbol{q}([U]/\boldsymbol{V_{rev}})^2}\right), \tag{42}$$

and i_{ep} is the current flowing through a single pore:

$$i_{ep}(v_m) = \frac{\pi \boldsymbol{r_m^2} \boldsymbol{\sigma} RT}{F\delta} \frac{v_m(\mathrm{e}^{v_m} - 1)}{\dfrac{\boldsymbol{w_0} \mathrm{e}^{\boldsymbol{w_0} - \boldsymbol{n} v_m} - \boldsymbol{n} v_m}{\boldsymbol{w_0} - \boldsymbol{n} v_m} \mathrm{e}^{v_m} - \dfrac{\boldsymbol{w_0} \mathrm{e}^{\boldsymbol{w_0} + \boldsymbol{n} v_m} + \boldsymbol{n} v_m}{\boldsymbol{w_0} + \boldsymbol{n} v_m}}, \tag{43}$$

with $v_m = [U] \times F/RT$ the adimensionalized transmembrane voltage.

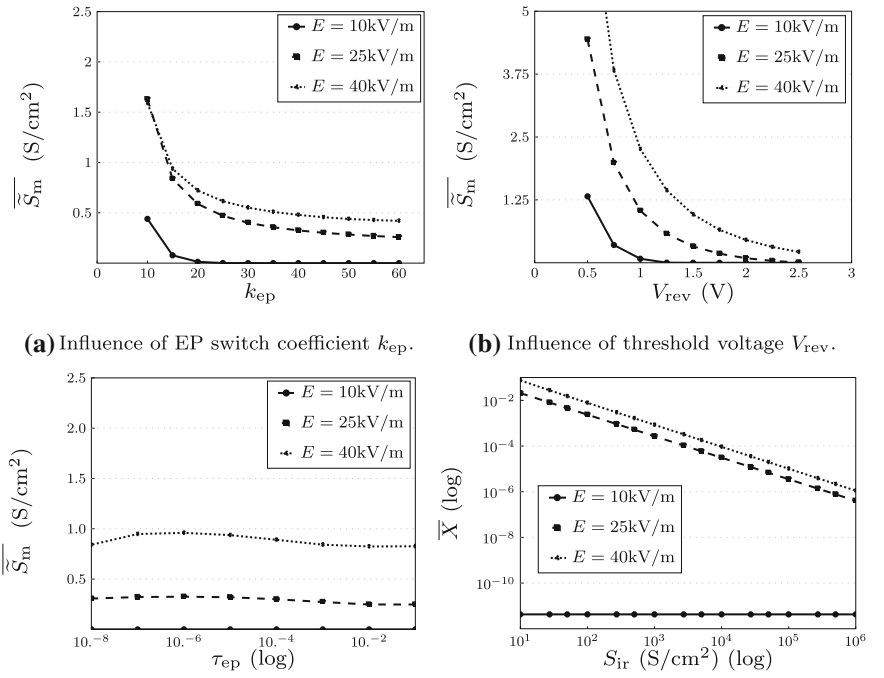

(a) Influence of EP switch coefficient $k_{\rm ep}$. **(b)** Influence of threshold voltage $V_{\rm rev}$.

(c) Influence of the characteristic time $\tau_{\rm ep}$. **(d)** Influence of the EPd surface conductivity $S_{\rm ir}$.

Fig. 7 Influence of each parameter on the mean value $\overline{\widetilde{S}_{\rm m}}$ of $\widetilde{S}_{\rm m}$ (**a**, **b**, **c**), and on the mean value $\overline{X}$ of X (**d**) at $t = 100$ µs. Three magnitudes of electric pulses are considered: 10, 25 and 40 kV/m

The numerical parameters for the model of Neu, Krassowska, et al. are those of Table 1 page 1215 of DeBruin and Krassowska (1999a). Our model reproduces qualitatively the behavior of ΔTMP as shown in Fig. 8. In Fig. 9, we show that the variation of the membrane current density $\widetilde{S}_{\rm m}[U]$ of our modeling is similar to the electroporation current density $N_{\rm ep} i_{\rm ep}$ of DeBruin and Krassowska (1999a).

4.4.4 Long-time behavior of the numerical solution to the dynamical model

In this paragraph, we compare the long-time behavior of the solution $U_{\rm dyn}$ to the dynamic model for a constant pulse with the solution $U_{\rm stat}$ to the static model.

Simulations are done in order to reach the time scale of the resealing characteristic time $\tau_{\rm vres}$ (Fig. 10). A constant pulse g is applied until the steady state of the dynamical system is reached. Observe that the stationary value of $\widetilde{S}_{\rm m}$, which is reached after about 500 µs is lower than the value of $\widetilde{S}_{\rm m}$ a few tens of microseconds after the beginning of the pulse delivery. For pulses of short duration, it is therefore important to simulate our new dynamical model instead of the steady model of Ivorra et al. (2010).

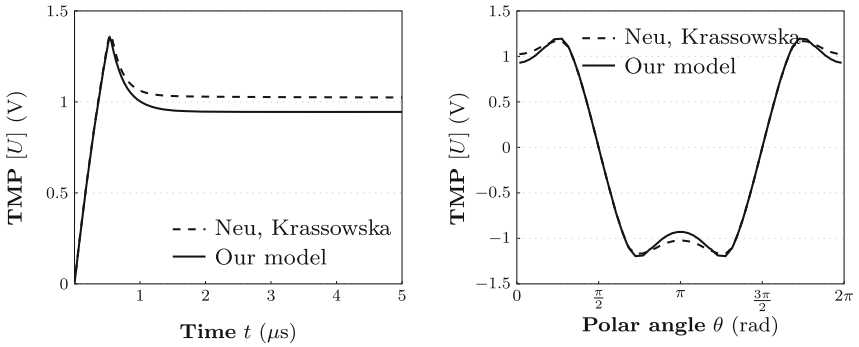

(a) Evolution of the ΔTMP at the cell's pole. **(b)** Values of the ΔTMP after 100 μs along the perimeter of the circular cell.

Fig. 8 Comparison of the ΔTMP obtained respectively with our model (*solid lines*) and with the model of Neu, Krassowska, et al. (*dashed*), with parameters from Table 1

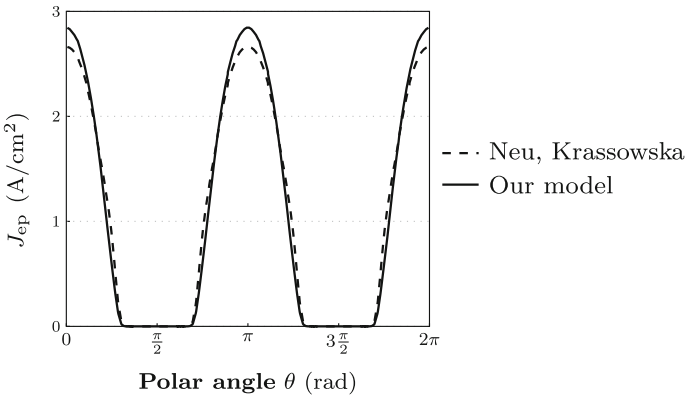

Fig. 9 Current density through the membrane of the model of Neu, Krassowska, et al., that is $J_{ep} = N_{ep} i_{ep}$ (in *dashed line*), compared with the membrane current density of our model (in *solid line*), $J_{ep} = \widetilde{S}_m [U]$, along the the cell membrane at 100 μs

Fig. 10 Averaged membrane conductivity $\widetilde{S}_m$ during long-time simulations. Steady state is reached after several hundreds of microseconds, which is larger than usual pulse duration

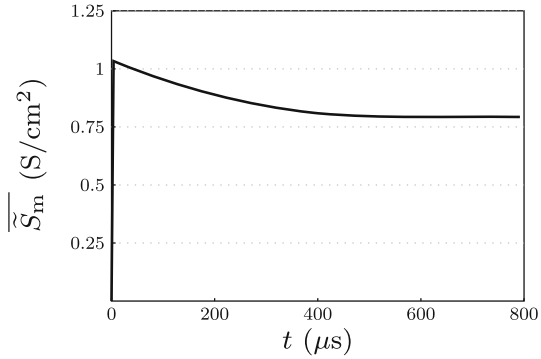

5 Conclusion

In this paper, we introduce two models describing the electropermeabilization of a single cell. We first study the static model, which is inspired by Ivorra et al., and we show existence and uniqueness results. We then derive a new dynamic model of cell electropermeabilization, which takes the permeabilizing time into account. We studied mathematical properties of this new model. We then provided an accurate finite-difference method on cartesian grid to compute these models, and we eventually presented numerical simulations for both static and dynamic models, that corroborate the results of the most achieved model of Neu, Krassowska, et al.

The main feature of our models lies in the fact that without loss of accuracy it is composed by a small number of parameters (mainly 4 parameters: S_{ir}, V_{rev}, and τ_{ep}, and τ_{vres} for the dynamical system) compared with the sophisticated models with tens of hardly measurable parameters of Neu, Krassowska, et al. Therefore, a forthcoming fitting of our models with the experimental data seems feasible, which is hardly the case for models with a large number of parameters.

From the biological point of view, we highlight the fact that the static model can be used for very long pulses (around 1 ms) but, for short pulses around 10 μs and below, the dynamics of the phenomenon have to be considered.

Acknowledgments The authors thank very warmly the biologists of the CNRS research team "UMR 8203 Vectorology and anti-cancerous therapeutics" at the Institut Gustave Roussy. Particulary, the discussions with Dr. A. Silve and Dr. L.M. Mir were very helpful in the understanding of the cell electropermeabilization.

References

André FM, Gehl J et al (2008) Efficiency of high- and low-voltage pulse combinations for gene electrotransfert in mucle, liver tumor and skin. Human Gene Therapy 19

Cisternino M, Weynans L (2012) A parallel second order cartesian method for elliptic interface problems. Commun Comput Phys 12

DeBruin K, Krassowska W (1999) Modelling electroporation in a single cell. I. Effects of field strength and rest potential. Biophys J 77:1213–1224

DeBruin K, Krassowska W (1999) Modelling electroporation in a single cell. II. Effects of ionic concentrations. Biophys J 77:1225–1233

Goldman DE (1943) Potential, impedance and rectification in membranes. J Gen Physiol 27:37–60

Gowrishankar TR, Esser AT, Vasilkoski Z, Smith KC, Weaver JC (2006) Microdosimetry for conventional and supra-electroporation in cells with organelles. Biochem Biophys Res Commun 341(4):1266–1276

Hodgkin AL, Katz B (1949) The effect of sodium ions on the electrical activity of the giant squid axon. J Physiol 108:37–77

Hodgkin L, Horowicz P (1959) The influence of potassium and chloride ions on the membrane potential of single muscle fibres. J Physiol 148:127–160

Hodgkin L, Huxley A (1952) A quantitative description of membrane current and its application to conduction and excitation in nerve. J Physiol 117:500–544

Ivorra A, Villemejane J, Mir LM (2010) Electrical modeling of the influence of medium conductivity on electroporation. Phys Chem Chem Phys 12(34):10055–10064

Marty M, Sersa G, Garbay J-R et al (2006) Electrochemotherapy—an easy, highly effective and safe treatment of cutaneous and subcutaneous metastases: Results of esope (European standard operating procedures of electrochemotherapy) study. Eur J Chem Suppl 3–13

Mir LM (2001) Therapeutic perspectives of in vivo cell electropermeabilization. Bioelectrochemistry 53: 1–10

Mir LM (2005) Electroporation of cells in tissues. Methods for detecting cell electropermeabilisation in vivo. In: Electroporation based technologies and treatment: proceedings of the international scientific workshop and postgraduate course, 14–20 November 2005. Ljubljana, Slovenia, pp 32–35

Neu J, Krassowska W (1999) Asymptotic model of electroporation. Phys Rev E 53(3):3471–3482

Neu J, Krassowska W (2006) Singular perturbation analysis of the pore creation transient. Phys Rev E 74(031917):1–9

Osher S, Sethian JA (1988) Fronts propagating with curvature-dependent speed: algorithms based on Hamilton–Jacobi formulations. J Comput Phys 79(12)

Pavlin M, Kotnik T, Miklavcic D, Kramar P, Lebar AM (2008) Electroporation of planar lipid bilayers and membranes. Adv Planar Lipid Bilayers Liposomes 6(7)

Perrussel R, Poignard C (2011) Asymptotic expansion of steady-state potential in a high contrast medium with a thin resistive layer. INRIA research report RR-7163. http://hal.inria.fr/inria-00442659/fr/

Pucihar G, Kotnik T, Valič B, Miklavčič D (2006) Numerical determination of transmembrane voltage induced on irregularly shaped cells. Ann Biomed Eng 34(4):642–652

Serša G (2005) Application of electroporation in electrochemotherapy of tumors. In: Electroporation based technologies and treatment: proceedings of the international scientific workshop and postgraduate course, 14–20 November 2005 Ljubljana, Slovenia, pp 42–45

Smith J, Neu K, Krassowska W (2004) Model of creation and evolution of stable electropores for DNA delivery. Biophys J 86:2813–2826

Teissié J (2005) In Vitro cell electropermeabilization. In: Electroporation based technologies and treatment: proceedings of the international scientific workshop and postgraduate course, 14–20 November 2005. Ljubljana, Slovenia, pp 29–31

Teissié J, Golzio M, Rols MP (2005) Mechanisms of cell membrane electropermeabilization: a minireview of our present (lack of?) knowledge. Biochim Biophys Acta 1724:270–280